Mon. Not. R. astr. Soc. (1969) **144**, 375–389.

THERMAL CONTINUUM RADIATION FROM CORONAL PLASMAS AT SOFT X-RAY WAVELENGTHS

J. L. Culhane

(Communicated by R. L. F. Boyd, F.R.S.)

(Received 1969 February 24)

SUMMARY

The continuous spectra, arising from the free–free and free–bound transitions of electrons in coronal plasmas, are calculated for wavelengths in the range 1 Å to 30 Å and at temperatures in the range 0·8 10^6 °K to 100·0 10^6 °K. The effect of variations in the element abundances is investigated. Estimates of the continuum flux from the solar corona are presented and the observed line to continuum ratios discussed.

1. INTRODUCTION

In a plasma, whose electrons have a Maxwellian velocity distribution, free–free and free–bound transitions of these electrons produce a continuous photon spectrum. This continuum radiation, at soft X-ray wavelengths, is of importance in the study of the solar corona and of other celestial X-ray sources.

Calculations of the continuous X-ray spectrum of the solar corona have been carried out by Elwert (1954). His calculations covered the wavelength range 1–100 Å and were carried out at selected temperatures in the range 0·8 10^6 °K to 100·0 10^6 °K. This work was extended by Kawabata (1960) to include additional values in the temperature range 10^7 °K to 10^8 °K. Calculations of the Coronal continuous spectrum have been carried out at temperatures below 2·8 10^6 °K by Widing (1966). Of these authors, only Widing has considered the effect of the dielectronic recombination process (Burgess private communication) on the ionization balance. Several calculations of the free–free spectrum from a hot plasma have been carried out (see for example Greene (1959) and Hovenier (1966)).

This paper presents calculations of the continous spectra emitted by a coronal plasma due to the free–free and free–bound processes. The calculations have been carried out for the wavelength range 1 to 30 Å and the temperature range 0·8 10^6 °K to 100·0 10^6 °K. The effect of variations in the element abundances on the spectra is investigated. Estimates of the continuum flux from the solar corona are presented and the observed line to continuum ratios discussed.

2. FREE–FREE RADIATION

The intensity of free–free or Bremsstrahlung emission, of frequency ν Hz, from unit volume of a plasma per second per unit frequency interval is given by

$$I = h\nu \sum_Z N_Z N_e \int_0^\infty d\sigma(v) f(v)\, dv \qquad (1)$$

$$\text{erg cm}^{-3}\,\text{s}^{-1}\,\text{Hz}^{-1}$$

where N_Z is the number of ions of charge Z and N_e is the number of electrons per unit volume, $d\sigma(v)$ is the cross section for the production of a photon of frequency ν by an electron of velocity v, $f(v)$ is the Maxwell velocity distribution function and h is Planck's constant.

Brussard & Van de Hulst (1962) have discussed the accuracy of various non-relativistic formulae for the calculation of the Bremsstrahlung flux from a Maxwellian plasma. Following their treatment, the flux from unit volume of the solar corona, at Earth distance, may be written as

$$\eta_{FF} = 7\cdot15.10^{-50}\, N_e \sum_Z N_Z Z^2 \exp\left[-\frac{143\cdot89}{\lambda T}\right] \frac{\bar{g}(Z, T, c/\lambda)}{T^{1/2}\,\lambda^2}\, d\lambda \quad \text{erg cm}^{-2}\,\text{s}^{-1}\,\text{Å}^{-1} \tag{2}$$

where λ is the photon wavelength in Å, T is the electron temperature in units of 10^6 °K and $\bar{g}(Z, T, c/\lambda)$ is a temperature average of the free–free Gaunt factor $g(Z, E, c/\lambda)$, a factor which expresses the difference between the classical and quantum mechanical cross sections for the free–free process. The temperature average is obtained by integrating over the Maxwellian distribution as shown in equation (3):

$$\bar{g}(Z, T, c/\lambda) = \exp\left[\frac{hc}{\lambda kT}\right] \int_{\frac{hc}{\lambda}}^{\infty} g(Z, E, c/\lambda) \exp\left[-\frac{E}{kT}\right] \frac{dE}{kT}. \tag{3}$$

In this equation, E is the electron energy and k is Boltzman's constant.

Karzas & Latter (1961) have computed the temperature averaged Gaunt factor as a function of photon energy with the electron temperature as a parameter. Values of $\bar{g}(Z, T, c/\lambda)$ were obtained from their results for the temperature range 0·8 to 100·0 10^6 °K and the wavelength range 1 to 30 Å.

A comparison of the free–free cross sections obtained by the use of the Born–Elwert formula with those obtained using a relativistic formula (Koch & Motz (1959), their equation 3BN multiplied by the Elwert factor) suggests that the non-relativistic cross section may be used with an accuracy of about 10 per cent for electron energies less than 30 KeV.

In the solar corona, the principal contribution to the free–free flux is from hydrogen and helium with smaller contributions from several other elements. If, following Hovenier (1966), we rewrite equation (2) in the form

$$\eta_{FF} = \sum_Z F(Z, T\lambda)\, N_Z N_e Z^2\, d\lambda \tag{4}$$

where

$$F(Z, T, \lambda) = 7\cdot15.10^{-50} \exp\left[-\frac{143\cdot89}{\lambda T}\right] \frac{\bar{g}(Z, T, c/\lambda)}{T^{1/2}\,\lambda^2} \tag{5}$$

then we may write, for a mixture of elements,

$$\eta_{FF} = F(1, T, \lambda)\, N_1 N_e \left[1 + \sum_Z \frac{\bar{g}(Z, T, c/\lambda)}{\bar{g}(1, T, c/\lambda)}\, Z^2 \frac{N_Z}{N_H}\right] d\lambda \tag{6}$$

where N_1 is the number of hydrogen ions per unit volume. The numerical value of the bracketed term in equation (6) will depend on the element abundance values that are used.

Values of $\bar{g}(1, T, c/\lambda)$ were obtained from the data of Karzas & Latter for all the values of wavelength and temperature at which the calculations were carried out. The variation of the ratio $\bar{g}(Z, T, c/\lambda)/\bar{g}(1, T, c/\lambda)$ was checked at a number of wavelengths and temperatures in the ranges 0·8 to 100·0 10^6 °K and 1 to 30 Å for the twelve elements listed in Table I. The variations found in the ratio of the Gaunt factors would lead to fluctuations of up to 20 per cent in the value of the bracketed term in equation (6). These fluctuations are similar to those noted by Hovenier who found variations of up to 15 per cent in this term.

Table I shows values of the bracketed term in equation (5) at a temperature of 5·0 10^6 °K and a wavelength of 5 Å. Two sets of element abundances were employed. For the corona the abundance values used are those of Pottasch (1967) and Jordan (1968). In cases where these results have disagreed, an average value

TABLE I

Dependence of free–free flux on element abundances

Element	Coronal abundances (Pottasch 1967; Jordan 1967)	Photospheric abundances (Goldberg *et al.* 1960)	$\frac{\bar{g}(Z, T, c/\lambda)Z^2}{\bar{g}(1, T, c/\lambda)}\frac{N_Z}{N_H}$ Coronal	Photospheric
H	10^6	10^6	—	—
He	2·0 10^5	1·45 10^5	1·124	0·810
C	400	600	0·017	0·030
N	60	100	0·005	0·009
O	300	1000	0·018	0·060
Ne	40	40	0·008	0·008
Mg	30	30	0·007	0·007
Si	50	40	0·012	0·010
S	20	20	0·006	0·006
Ar	4*	4*	0·002	0·002
Ca	2*	2*	0·001	0·001
Fe	50	5	0·051	0·005
		Total	1·250	0·950

Note

Cosmic abundance of neon is 300 on the above scale (Allen (1963)). The set of abundances referred to as photospheric (2) is identical to the photospheric (1) set except that the cosmic value is used for neon. Values in columns 4 and 5 refer to a temperature of 5·0 10^6 °K and a wavelength of 5 Å.

* Cosmic abundance (Allen (1963)).

was taken but the disagreement is usually less than a factor of two. The calculations were also carried out using the Photospheric abundance values of Goldberg, Muller & Aller (1960). The abundance values used are listed in Table I. Those values marked with an asterisk are the cosmic abundance values quoted in Allen (1963). The value of the bracketed term, given in Table I for the coronal abundances, is about 25 per cent greater than the value for the photospheric abundances, but this difference is very sensitive to a small change in the abundance of helium.

Following Pottasch (1964), a helium to hydrogen ratio of 0·2 has been assumed for the corona while the cosmic abundance value of 0·15 has been taken for the photosphere.

For a given set of element abundances, the most significant error in the calculations arises from the method of summing the contributions of the various elements.

As stated above, this is probably less than 20 per cent. Where possible, values of the free–free flux, calculated using equation (6), were compared with the calculations of Hovenier. The agreement was found to be better than 15 per cent.

3. FREE–BOUND RADIATION

When a free electron, of kinetic energy E, is captured into a bound state of an ion, a photon is emitted of frequency

$$\nu = \frac{E+X_n}{h} \tag{7}$$

where X_n is the ionization potential of the electron after capture and n is the principal quantum number of the shell into which the electron has been captured. In this process the photon energy is a function only of the electron energy. In addition, only photons of energy greater than X_n can result from recombination into the nth shell. This causes discontinuities or recombination limit features in the free–bound spectrum emitted by an ion.

For hydrogen like ions, the flux from unit volume of the solar corona, as seen at Earth, may be written

$$\eta_{\mathrm{FB}} = 6{\cdot}01\ 10^{-53}\, N_1 N_e \exp\left[-\frac{143{\cdot}89}{\lambda T}\right] \underbrace{\sum}_{\text{Element}} \frac{N_{\mathrm{EL}}}{N_1} \underbrace{\sum}_{\text{Ionization stage}} \frac{N_{i+1}}{N_{\mathrm{EL}}} \frac{G\,d\lambda}{\lambda^2 T^{1.5}}$$

$$\text{erg cm}^2\,\text{s}^{-1}\,\text{Å}^{-1} \tag{8}$$

where

$$G = \sum_{n=n_0}^{\infty} \frac{\rho_n X_{i,\,n}{}^2}{n} \exp\left[\frac{0{\cdot}012\, X_{i,\,n}}{T}\right] g\left(Z, n, \frac{c}{\lambda}\right). \tag{9}$$

In these two equations, symbols that are common with equation (2) have the same meanings and units but, in addition, ρ_n is the number of positions in the nth shell which are free to be occupied by the captured electron, $X_{i,\,n}$ is the ionization potential of an electron in the nth shell of an ion of ionization stage i and $g(Z, n, c/\lambda)$ is the free–bound Gaunt factor. The ionization potential is in electron volts. N_{EL}/N_1 is the element abundance relative to hydrogen and at a given temperature, N_{i+1}/N_{EL} is the fraction of an element in the $(i+1)$th stage of ionization. This formula is similar to the one discussed by Brussard & Van de Hulst and others for the recombination of electrons with the $(i+1)$th stage of a hydrogen like ion. However, the hydrogen like expression for the ionization potential has been replaced, for each ion, by the explicit value $X_{i,\,n}$.

For each ion, contributions to the free–bound flux due to electron captures to all levels must be included as shown by the sum in equation (9). Here the n_0th level is the lowest level to which recombination is allowed for a given photon energy. For each element, the sum in equation (8) $(\Sigma N_{i+1}/N_{\mathrm{EL}})$ must include all the ionization stages that have a significant abundance at a given temperature. Values of the ratio N_{i+1}/N_{EL} greater than $3 \cdot 10^{-4}$ have been included in the calculations.

Values of the free–bound Gaunt factor $g(Z, n, c/\lambda)$ were obtained from the work of Karzas & Latter. Values of the Gaunt factor averaged over the sub-levels of each principal level were employed.

The ratio of the number of ions in the $(i+1)$th state to the number in the ith state is, under coronal conditions, given by

$$\frac{N_{i+1}}{N_i} = \frac{q_C + q_A}{\alpha_R + \alpha_D}. \tag{10}$$

Where q_c and q_A are the rate coefficients for collisional ionization and autoionization while α_R and α_D are the rate coefficients for radiative and dielectronic recombination.

The elements and ionization stages, which were considered in the present calculation, are listed in Table II. Values of log $(N_i/N_{\rm EL})$ for all the elements in Table II, except calcium, have been calculated by Jordan (1969) for temperatures in the range 10^4 °K to 10^8 °K, though the majority of the elements are fully stripped at temperatures above 10^7 °K. Ionization equilibrium calculations for calcium were carried out by Burgess & Faulkner (private communications) over the temperature range $1\cdot0\ 10^6$ to $2\cdot0\ 10^7$ °K.

TABLE II

Elements and ionization stages

Element	Range of ionization stages
H	I
He	II
C	IV–VI
N	V–VII
O	V–VIII
Ne	V–X
Mg	V–XII
Si	V–XIV
S	VI–XV
Ar	VII–XVIII
Ca	IX–XX
Fe	VI–XXV

The effect of autoionization was not included in the calculations. Its importance has been discussed by Goldberg, Dupree & Allen (1965) and by Van Rensbergen (1967) who find that for Fe XV, $q_A \simeq q_c$ for temperatures around $4\cdot0.10^6$ °K. In the case of other ions considered by these authors, $q_A \lesssim 0\cdot1\ q_c$ in the temperature range of interest here. Equilibrium calculations for iron have recently been carried out by Bely (1967). It is shown that autoionization is of considerable importance for ionization stages above Fe XV. However, as will be seen in the next section the contribution of iron to the total free–bound flux is never very large and at temperatures above 2–3 10^7 °K where the flux of recombination radiation from iron does become significant, the total free–bound flux becomes less important than the free–free flux.

For each ion, the sum over n in equation (9) was carried out term by term for values of n in the range $n = n_0$ to $n = 15$. In each case, values of $X_{i,\ n_0}$ were obtained from Allen (1963). Where possible, values of $X_{i,\ n}$ for $n > n_0$ were obtained from the term value tables of Moore (1949, 1952). When this was not possible, hydrogen like values of $X_{i,\ n}$ were calculated using an effective value of Z^2 in the hydrogen like expression for the ionization potential. This procedure probably underestimates the value of $X_{i,\ n}$. However, the first term of the sum in equation

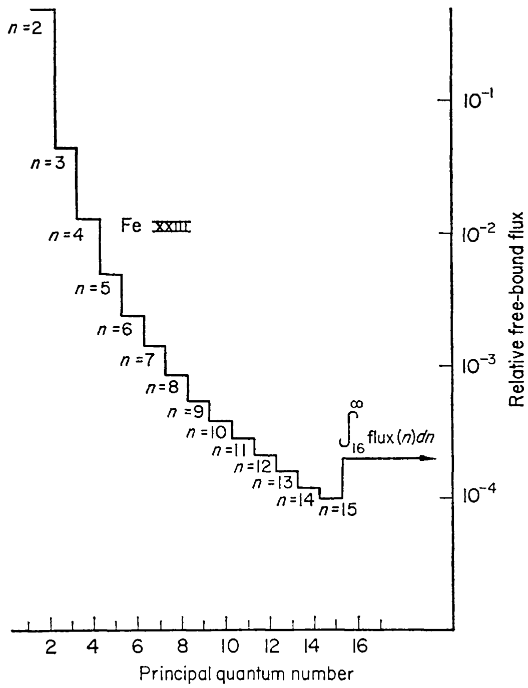

FIG. 1. *Relative fluxes due to recombination in Fe* XXIII.

(9) is the most significant. This is shown in Fig. 1 where the flux produced by recombination to each level is plotted against n for the ion Fe XXIII.

For values of n greater than or equal to 16, the summation in equation (9) was replaced by integration with $X_{i,\,n}$ being taken as the hydrogen like expression for ionization potential X_n, where

$$X_n = \frac{2\pi^2 m Z^2 e^4}{h^2 n^2}. \tag{11}$$

Using this expression for X_n, we may write

$$\sum_{16}^{\infty} \frac{\beta^2 Z^4}{n^3} \exp\left[\frac{0\cdot012\,\beta Z^2}{Tn^2}\right] \simeq \int_{16}^{\infty} \frac{\beta^2 Z^4}{n^3} \exp\left[\frac{0\cdot012\,\beta Z^2}{Tn^2}\right] dn \tag{12}$$

where

$$\beta = \frac{2\pi^2 m e^4}{h^2} \tag{13}$$

and the Gaunt factor is set equal to unity. The value of the flux derived from the use of the integral in equation (12) is shown in Fig. 1.

4. CONTINUUM CALCULATIONS

Calculations of the free–free and free–bound fluxes, emitted by Maxwellian plasmas, were carried out for temperatures in the range $0\cdot8\ 10^6$ °K to $100\cdot0\ 10^6$ °K and for wavelengths in the range 1 to 30 Å. The formulae described in the previous sections were employed. As discussed in Section 2, the free–bound calculations were carried out by summing the terms in equation (9) up to a value of $n = 15$. The contributions for $n = 16$ to $n = \infty$ were estimated using the integral from equation (12). The magnitude of the terms in this summation are shown in Fig. 1 for the case of Fe XXIII.

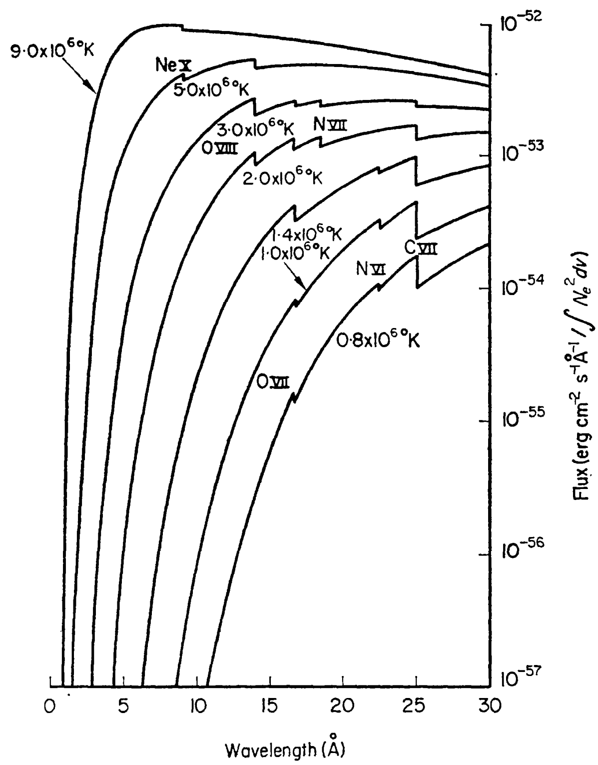

FIG. 2. *Free–free and free–bound fluxes for* $T < 10^7$ *°K.*

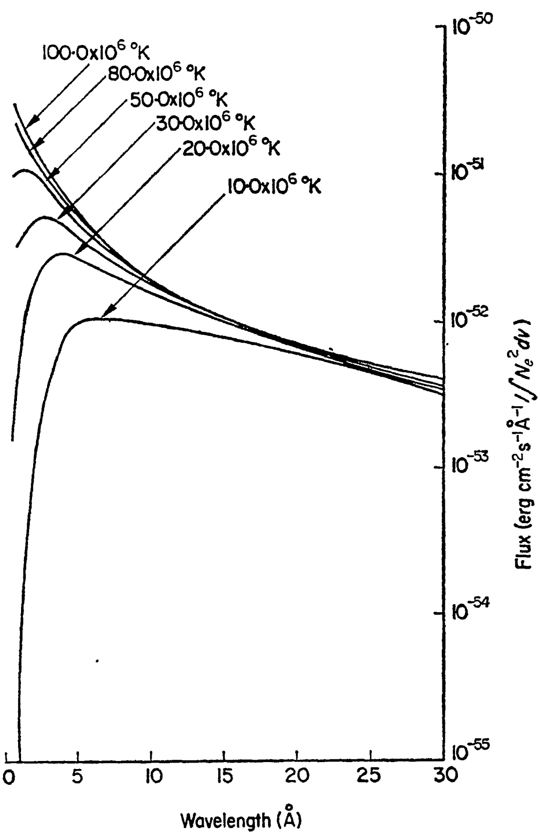

FIG. 3. *Free–free and free–bound fluxes for* $T > 10^7$ *°K.*

The spectra resulting from both free–free and free–bound process are shown in Figs 2 and 3 for various temperatures. The coronal abundances, listed in Table I, were used to calculate these spectra.

The recombination limits of several ionization stages may be seen in the spectra, but with the possible exception of the C VI limit above 25 Å, these features are not very significant and would, therefore, be difficult to observe in the solar spectrum. Crystal spectrometer observations of the quiet Sun (Fritz *et al.* 1967; Rugge & Walker 1967; Evans & Pounds 1968) have not shown any recombination limit features in the wavelength range below 25 Å, with the possible exception

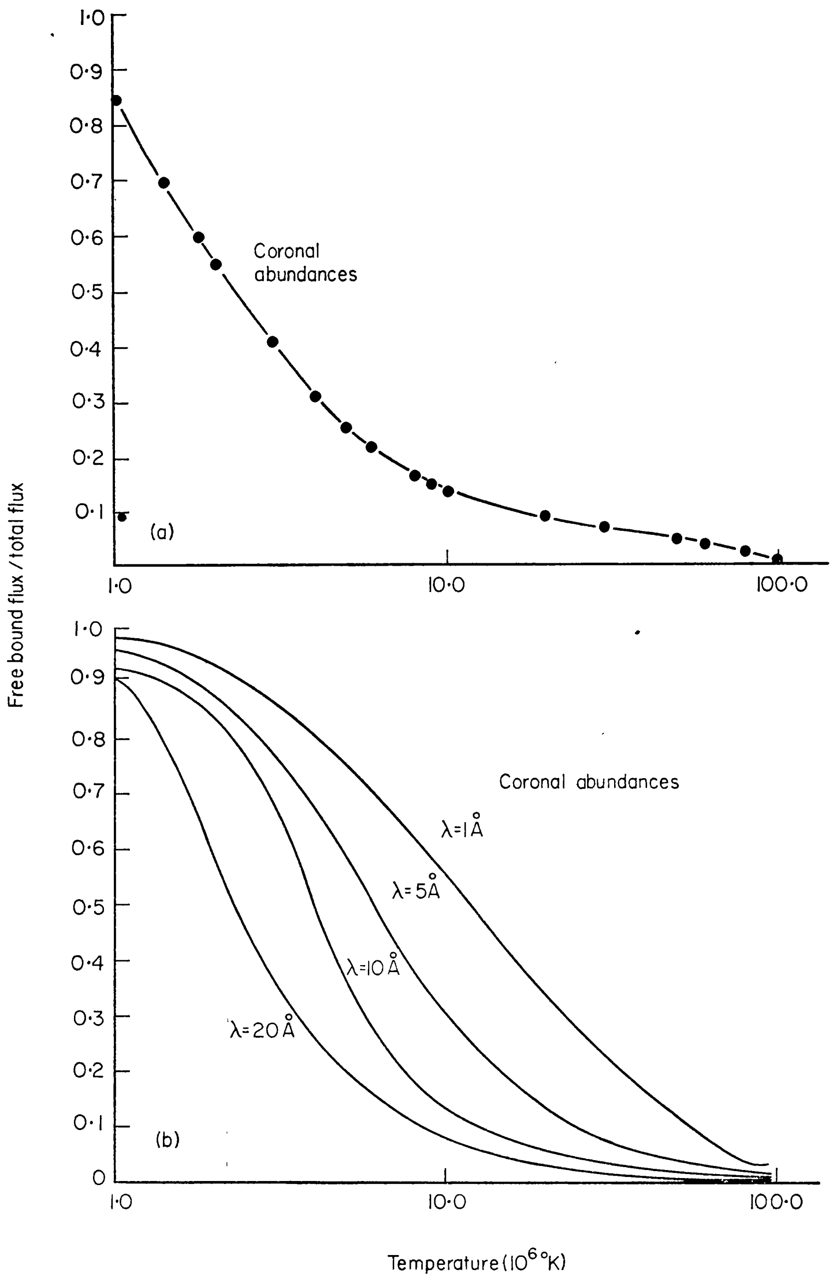

FIG. 4. (a) *Variation of the free–bound contribution to the total continuum flux in the wavelength range* 1 *Å to* 30 *Å.* (b) *Variation of the free–bound contribution to the total continuum flux at various wavelengths.*

of the identification of the N VII limit at 18·63 Å by Fritz *et al.* In particular, none of these spectra show the recombination limits of O VII or O VIII. Recent crystal spectrometer observations of solar flare spectra (Neupert *et al.* (1967), Meekins *et al.* (1968)) have also failed to show recombination limit features even though Meekins *et al.* find continuum to line ratios of 10 to 100 in the wavelength range below 8 Å during solar flares.

The contribution of the free–bound flux to the total flux is shown in Fig. 4(a). At temperatures greater than $20 \cdot 0 . 10^6$ °K, the free–bound process contributes less than 10 per cent of the total continuum flux in the wavelength range 1–30 Å.

The importance of the free–bound process also depends on wavelength. This is illustrated in Fig. 4(b) where the ratio of free–bound flux to total flux is plotted

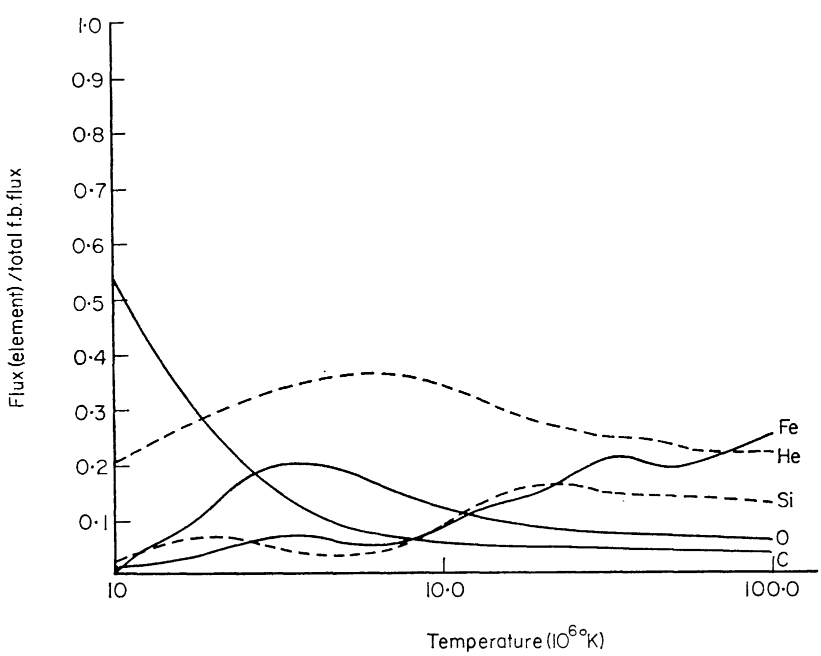

FIG. 5. *Contributions to the free–bound flux from various elements (coronal abundances).*

against temperature for four wavelengths in the range 1 Å to 30 Å. At short wavelengths the free–bound process remains the major contributor to the total continuum flux up to quite high temperatures. At longer wavelengths the dominance of the free–free process is established more quickly.

Fig. 5 shows the fraction of the free–bound flux, contributed by some of the elements, plotted against temperature. Although hydrogen is the most abundant element, its contribution to the free–bound flux is always less than 8 per cent in the 1–30 Å range because of its low atomic number. Helium remains a significant contributor over the whole temperature range, but does not have recombination limits at short wavelengths. With the exception of carbon, no other element makes a dominant contribution to the free–bound flux and, hence, absorption limits are not prominent features of the continuous spectra. Although the contribution of iron is becoming important at temperatures above $30 \cdot 0 \; 10^6$ °K, the free–free process is the major source of continuous flux at these temperatures and so iron recombination features do not appear.

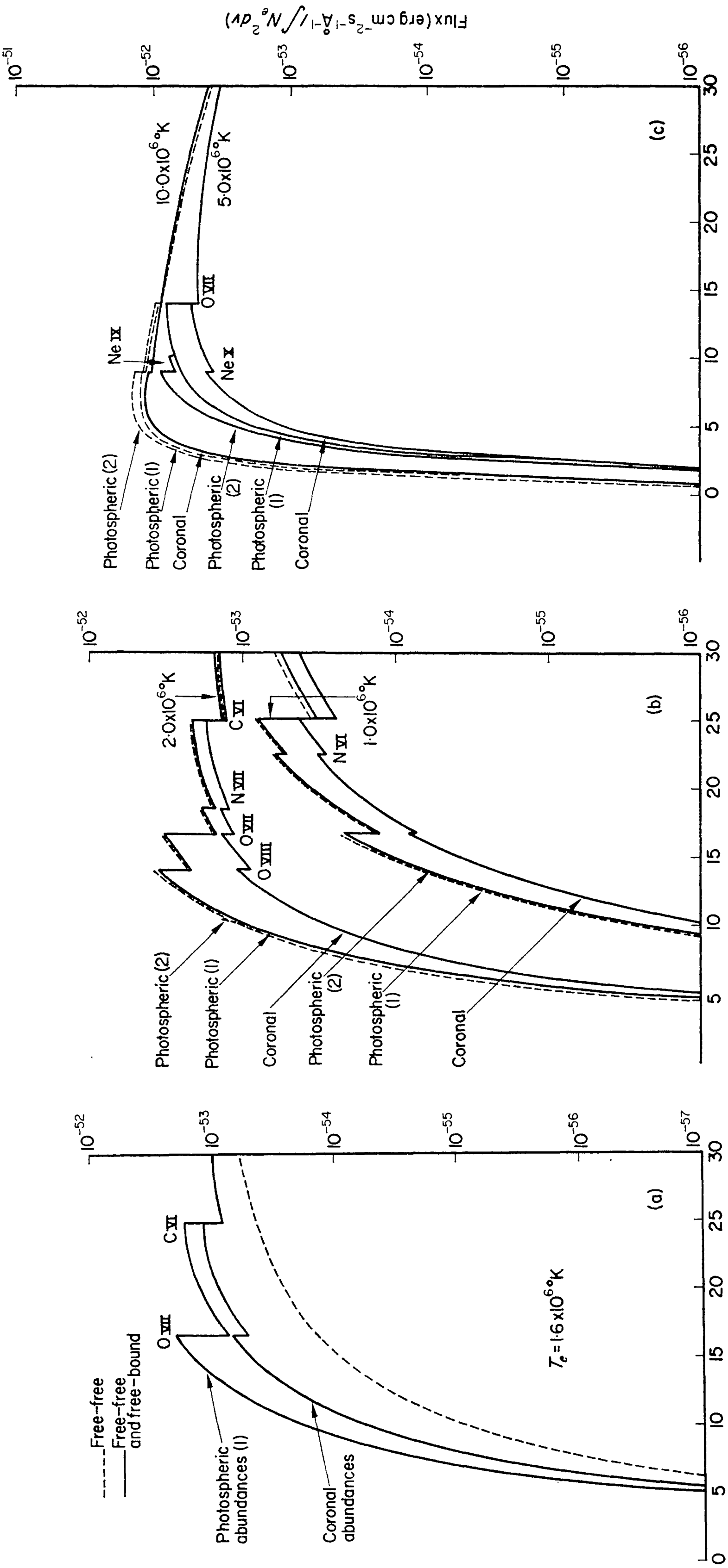

FIG. 6. (a) *The effect of element abundance on the continuum flux.*
(b) *The effect of element abundance on the continuum flux.*
(c) *The effect of element abundance on the continuum flux.*

5. THE EFFECT OF CHANGES IN THE ELEMENT ABUNDANCES ON THE CONTINUUM FLUX

The flux of free–free radiation is not greatly affected by the values of element abundance used in the calculation. This is evident from the constants listed in the last two columns of Table I. The two numbers quoted are the factors by which the free–free flux is increased relative to the flux from a hydrogen plasma. The difference between these factors amounts to only 25 per cent and is almost entirely due to the change in helium abundance.

At temperatures below $20 \cdot 0\ 10^6$ °K the contribution of the free–bound process becomes a significant and, at lower temperatures, the dominant source of continuum radiation. However, the amount of radiation contributed by an ion depends also on its abundance in the plasma and so the abundance values used in a continuum calculation can affect the result considerably.

Fig. 6(a) shows the calculated free–free and free–bound spectra for a temperature of $1 \cdot 6\ 10^6$ °K. Coronal abundances and photospheric abundances including the coronal value for neon have been used. As remarked in the previous section, the C VI limit is the only significant feature in the spectrum when the coronal abundances are used. This feature is enhanced if photospheric abundance values are employed. In addition, the greater oxygen abundance in the photospheric list enhances the limit features that are due to oxygen ions. The continuous spectrum calculated by Widing (1966) at a temperature of $1 \cdot 5\ 10^6$ °K was based on a similar set of abundances to those listed in Table I (photospheric (1)). This spectrum shows larger discontinuities at the C VI and O VII absorption limits than the spectrum shown in Fig. 6(a). However, the free–free spectrum calculated by Widing refers to a hydrogen plasma. If his free–free spectrum is increased to allow for the inclusion of other elements, the differences between the absorption limit features in his spectrum and those in the spectrum of Fig. 6(a) become considerably less.

Fig. 6(b) and (c) show continuous spectra that have been calculated using the three sets of element abundances referred to in Table I. All the spectra in these figures give the totals from the free–free and free–bound process. The difference between the spectra obtained using coronal and photospheric (1) abundances remains significant up to temperatures in excess of $5 \cdot 0\ 10^6$ °K. The use of the cosmic neon abundance (photospheric (2)) is quite noticeable at $5 \cdot 0\ 10^6$ °K. However, at $10 \cdot 0\ 10^6$ °K the importance of the free–bound process is diminishing and the effect of variations in element abundances becomes less significant.

6. EMISSION FROM THE SOLAR CORONA

Solar images have been obtained at soft X-ray wavelengths with pinhole cameras (Blake *et al.* (1963), Pounds & Russell (1966)) and grazing incidence reflecting telescopes (Underwood & Munie 1967; Vaiana *et al.* 1968). These observations show that X-radiation at wavelengths below 20 Å comes almost entirely from small sources in the corona. These sources lie above calcium plages. Radiation at longer wavelengths is produced throughout the corona and exhibits limb brightening. The crystal spectrometer observations of Evans & Pounds (1968) and others suggest that the general coronal temperature is less than $1 \cdot 6\ 10^6$ °K while the temperature of individual X-ray active regions may be as high as 4 to 5 10^6 °K. Higher temperatures are also required to explain the continuum emission from

X-ray active regions at wavelengths below 7 Å (Culhane *et al.* (1969)). The spectral and spatially resolved observations at present available do not allow the determination of temperature structure in either the general corona or in individual active regions. It is likely that the quiet corona contains material at temperatures in the range $1 \cdot 2$–$5 \cdot 0 \; 10^6$ °K. Models which suggest two or three regions at different fixed temperatures are probably unrealistic, but they do allow an estimate of the temperature extremes involved and a check on the validity of the hypothesis that the soft X-radiation from the quiet corona is due to thermal emission.

The parameters of the model that Evans & Pounds deduce from their results are summarized in Table III. Their model (model (1)) describes the general corona and one active region. The model (2) parameters are based on proportional counter observations of the quiet Sun at wavelengths below 10 Å (Culhane *et al.* (1969)). They refer to the whole Sun. The value of the mean emission measure for the general coronal radiation, deduced by Evans & Pounds from their O VII line observations, is lower than values based on coronal electron density estimates. The general coronal emission measure for model (2) has, therefore, been taken as $3 \cdot 0 \; 10^{49}$ (Elwert 1961).

TABLE III

Coronal models

No.	Temperature (°K)	Emission measure (cm^{-3})	Remarks	Source
1	$1 \cdot 5 \; 10^6$	$1 \cdot 5 \; 10^{49}$	General corona and one active region	Evans & Pounds (1968)
	$3 \cdot 0 \; 10^6$	$1 \cdot 7 \; 10^{48}$	Crystal spectrometer observations on 1966 May 5, 2800 MHz flux was 90 units	—
	$4 \cdot 0 \; 10^6$	$1 \cdot 0 \; 10^{47}$		
2	$1 \cdot 5 \; 10^6$	$3 \cdot 2 \; 10^{49}$	General corona	Elwert (1961)
	$3 \cdot 0 \; 10^6$	$5 \cdot 0 \; 10^{48}$	X-ray active region emission from whole Sun. Proportional counter observation 1967 November 8, 2800 MHz flux was 110 units	Culhane *et al.* (1969)
	$5 \cdot 0 \; 10^6$	$1 \cdot 7 \; 10^{47}$		

Continuous spectra have been calculated using the parameters in Table III. The coronal abundance values from Table I were employed. The spectra are plotted in Fig. 7 where they are labelled model (1) and model (2). The line intensities measured by Evans & Pounds on 1966 May 5 are given in Table IV. The line fluxes are totalled in 2 Å intervals and refer to the whole Sun, although the major contribution to the higher excitation lines is from one active region.

If we regard the two continuous spectra as providing upper and lower limits to the thermal continuum radiation, then the line to continuum ratios, derived from the data in Fig. 7, are given in Table IV. The model (2) continuous spectrum is probably too intense to be reasonably compared with the line intensity obtained by Evans & Pounds, since it refers to a measurement made more than a year after their results were obtained. Although the data of Culhane *et al.* were obtained on 1967 November 8 during quiet solar conditions, the 2800 MHz radio flux was 110 units. On 1966 May 5, the radio flux value was 90 units. The fact that the lower limit for the line to continuum ratio, measured by Evans & Pounds,

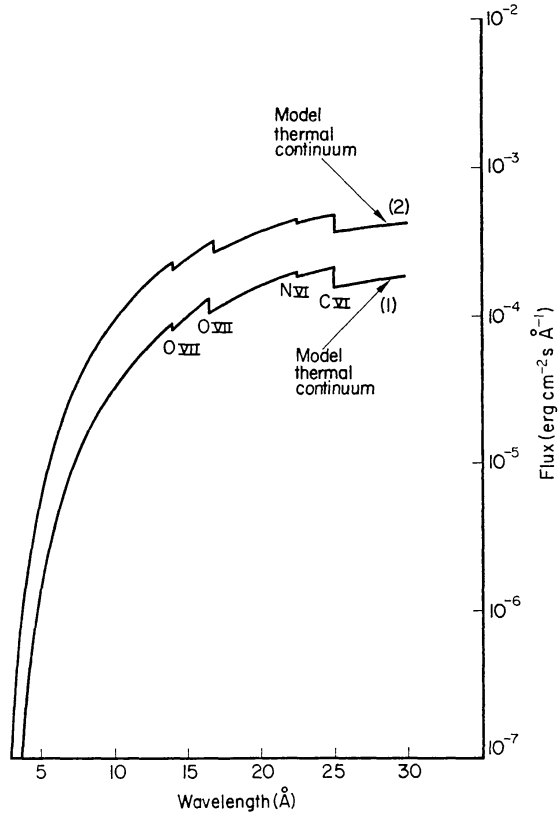

FIG. 7. *Continuum emission from the solar corona.*

was 9·0, also suggests that the model (2) continuous spectrum has too large a flux.

The calculated continuous spectra indicate that, if the soft X-ray flux from the quiet Sun is mainly due to thermal continuum emission from active regions in the 3·0–5·0 10^6 °K temperature range, then the continuum should not be registered by the crystal spectrometers of about 1 cm^2 collecting area that are currently employed to observe the solar X-ray spectrum. The results of Evans & Pounds and of Rugge & Walker (1967) support this conclusion, since they do not indicate continuum flux. In addition, recombination limit features in the spectrum should be small and not easily observable if the element abundances are coronal (see Table I).

TABLE IV

Line to continuum ratios

Wavelength interval ($\Delta\lambda$ Å)	Total continuum flux (erg cm^{-2} s^{-1} $\Delta\lambda^{-1}$) Model 1	Model 2	Line flux (erg cm^{-2} s^{-1} $\Delta\lambda^{-1}$) (Evans & Pounds)	Line to continuum ratio Model 1	Model 2	Lower limit (Evans & Pounds)
12–20	8·7 10^{-4}	2·1 10^{-3}	13·4 10^{-3}	14·3	6·3	9·0
12–14	1·5 10^{-4}	3·7 10^{-4}	8·8 10^{-4}	5·9	2·4	—
14–16	2·0 10^{-4}	4·8 10^{-4}	2·3 10^{-3}	11·1	4·8	—
16–18	2·5 10^{-4}	6·0 10^{-4}	2·2 10^{-3}	9·1	3·7	—
18–20	2·8 10^{-4}	6·8 10^{-4}	2·4 10^{-3}	8·4	3·6	—
20–22	3·5 10^{-4}	8·0 10^{-4}	5·6 10^{-3}	16·6	7·2	—

The solar spectrum has also been observed under quiet conditions by Fritz *et al.* (1967). They used two crystal spectrometers to cover the wavelength ranges 1·7 Å to 8·3 Å and 5 Å to 25 Å. Their observations suggest a line to continuum ratio of 0·5 in the wavelength range 10 Å to 20 Å. If the processes involved are purely thermal, the line to continuum ratio should, as demonstrated above, be much larger than this. Additional continuum radiation could be provided by the interactions of non-thermal electrons with the ions in the plasma.

7. CONCLUSIONS

The continuous spectra arising from the free–free and free–bound processes in a coronal plasma have been calculated for temperatures in the range 0·8 10^6 °K to 100·0 10^6 °K. The formulae employed in these calculations are discussed in Sections 2 and 3.

Although the free–bound process is the dominant source of continuum radiation at temperatures below 10·0 10^6 °K, absorption limit features are not prominent when coronal abundances (Pottasch 1967; Jordan 1968) are used in the calculations.

The flux of free–free radiation is not greatly affected by changes in element abundance although it is affected slightly by changes in the helium abundance. The use of the photospheric abundance of Goldberg *et al.* (1960) in the continuum calculation enhances the recombination limit features due to C VI, O VII and O VIII. Features due to N VI and N VII also become more pronounced. If the cosmic value for the abundance of neon is used in place of the coronal value, features due to Ne IX and Ne X become significant at temperatures above 4·0 10^6 °K.

The soft X-ray emission from the solar corona at wavelengths below 15 Å, comes mainly from localized active regions. The observations of Evans & Pounds and others suggest that these regions are hotter than the general corona. If the radiation is due to thermal process alone, in both the active regions and the general corona, then the continuous spectrum would not be registered by the crystal spectrometers currently in use. Most of the crystal spectrometer observations fail to show the continuous spectrum. The observation of Fritz *et al.* (1967) suggests that, on some occasions, there is an additional source of continuum radiation.

ACKNOWLEDGMENTS

The author is grateful to Professor R. L. F. Boyd for his support and encouragement. He has also benefitted from discussions with Dr A. Burgess and Dr C. Jordan and acknowledges their assistance with gratitude.

Mullard Space Science Laboratory, Physics Department, University College, London.

REFERENCES

Allen, C. W., 1963. *Astrophysical Quantities*, 2nd edn, Athlone Press, London.
Bely, O., 1967. *Ann. d'Astrophys.*, **30**, 953.
Blake, R. L., Chubb, T. A., Friedman, H. & Unzicker, A. E., 1963. *Astrophys. J.*, **137**, 3.
Brussard, P. J. & Van de Hulst, H. C., 1962. *Rev. mod. Phys.*, **34**, 507.
Burgess, A., 1964. *Astrophys. J.*, **145**, 380.

Culhane, J. L., *et al.*, 1969. *Mon. Not. R. astr. Soc.*, in press.
Elwert, G., 1954. *Z. Naturf.*, **9a**, 637.
Elwert, G., 1961. *J. geophys. Res.*, **66**, 391.
Evans, K. & Pounds, K. A., 1968. *Astrophys. J.*, **152**, 319.
Fritz, G., Kreplin, R. W., Meekins, J. F., Unzicker, A. E. & Friedman, H., 1967. *Astrophys. J.*, **144**, L133.
Goldberg, L., Muller, E. A. & Aller, L. H., 1960. *Astrophys. J.*, Suppl. Ser., **5**, No. 45, 1–137.
Goldberg, L., Dupree, A. K. & Allen, J. W., 1965. *Ann. d'Astrophys.*, **28**, 589.
Greene, J., 1959. *Astrophys. J.*, **130**, 693.
Hovenier, J. W., 1966. *Bull. astr. Insts Neth.*, **18**, 185.
Jordan, C., 1968. Private communication.
Jordan, C., 1969. *Mon. Not. R. astr. Soc.*, **142**, 501.
Karzas, W. J. & Latter, R., 1961. *Astrophys. J.*, Suppl. Ser., **6**, 167.
Kawabata, Kin-Aki, 1960. *Rep. ions space Res. Japan*, **14**, 405.
Koch, H. W. & Motz, J. W., 1959. *Rev. mod. Phys.*, **31**, 920.
Meekins, J. F., Kreplin, R. W., Chubb, T. A. & Friedman, H., 1968. Submitted to *Science* for publication.
Moore, C. E., 1949. *Atomic Energy Levels, I.* NBS Circular No. 467.
Moore, C. E., 1952. *Atomic Energy Levels, II.* NBS Circular No. 467.
Neupert, W. M., Gates, W., Swartz, M. & Young, R., 1967. *Astrophys. J.*, **144**, L133.
Pottasch, S. R., 1967. *Bull. astr. Insts Neth.*, **19**, 113.
Pottasch, S. R., 1964. *Space Sci. Rev.*, **3**, 816.
Pounds, K. A. & Russell, P. C., 1966. *Space Res.*, **6**, 34.
Rugge, H. & Walker, A. B. C., 1967. *Space Res.*, **8**, 439.
Underood, J. H. & Munie, W. S., 1967. *Solar Phys.*, **1**, 129.
Vaiana, G. S., Reidy, W. P., Zehnpfennig, T., Van Speybroeck, L. & Giaconni, R., 1968. *Science*, **161**, 564.
Van Rensbergen, W., 1967. *Bull. astr. Insts Neth.*, **19**, 6.
Widing, K., 1966. *Astrophys. J.*, **145**, 380.